Interaction of hydrogen with substitutional and interstitial carbon defects in silicon

P. Leary and R. Jones
Department of Physics, University of Exeter, Exeter EX4 4QL, United Kingdom

S. Öberg
Department of Mathematics, University of Luleå, Luleå, S95 187, Sweden

(Received 14 July 1997)

An *ab initio* cluster method is used to investigate substitutional, C_s, and interstitial, C_i, carbon defects in silicon complexed with hydrogen. We find that the binding energy of neutral H with C_s is 1.01 eV, and that the defect is bistable. In the positive and neutral charge states H lies near the center of a C-Si bond, and is antibonded to C in the negative charge state. A second H atom can be trapped in a H_2^* defect. H forms stronger bonds with interstitial C_i. In the C_i-H defect, the binding energy of H is 2.8 eV, and two low-energy structures have almost degenerate energies. These consist of a bond-centered Si-(C_i-H)-Si defect and a $\langle 100 \rangle$-oriented C_i-Si split interstitial with H bonded to C_i. The calculated barrier for conversion between the two stable structures is very low, ~ 0.3 eV, implying that the defect migrates rapidly, and readily reacts with other defects or impurities present. Two possible reactions are considered: the first is with another H and the second with C_s. The defect is completely passivated in the former while the stable form of the latter consists of a $\langle 100 \rangle$ C-C dicarbon interstitial, where one radical is passivated by H. The calculated symmetry and the local vibrational modes are in excellent agreement with those experimentally observed for the *T* photoluminescent center. Finally, a further reaction involving the *T* center and a second H atom is considered, and is found to lead to the elimination of electrical activity. [S0163-1829(98)02707-6]

I. INTRODUCTION

Both carbon and hydrogen can be adventitious impurities in silicon. The former is introduced from graphitic contaminants or carbonaceous gases present during growth, while the latter may be introducing during processing or from water vapor. The carbon concentration is typically at least 5×10^{15} cm^{-3},[1] while the concentration of H is often unknown. The solubility of C is $\sim 4 \times 10^{17}$ cm^{-3} at the melting point of silicon,[2] and that of H is $\approx 10^{16}$ cm^{-3} at 1300 °C.[3] The two impurities have quite different properties: C is usually is a substitutional defect, C_s, which is electrically inert and immobile, while H is an interstitial defect. Although an isolated H interstitial is highly mobile and reactive, a pair of hydrogen atoms as in a molecule is inert. A single H atom can be trapped by C_s producing a defect which is electrically active, although of low thermal stability. This defect has been associated with the $E3$ and $H1$ levels detected by deep-level transient spectroscopy (DLTS).[4] Of greater stability is the defect formed when two H atoms are trapped as in a molecule or H_2^* near C_s—although there is no evidence for these latter defects at present.

Although C_s is the normal species of carbon, an interstitial form C_i is a prominent product formed after irradiation. This, like H, is electronically active and highly mobile and readily complexes with a large number of other centers, for example C_s and oxygen. Often these complexes are themselves electrically active and stable to quite high temperatures. We shall explore in this paper the defects formed by the reaction of C_s and C_i with H interstitials. Other defects involving C, H, and O will be discussed in a separate paper.

The simplest defect is C_iH, and it would be expected that this might be easily detected in proton-implanted Si containing C. However, we find it to be highly mobile and likely to rapidly react with C_s and/or H. One of the products, C_iC_sH, has been identified[5] as a photoluminescent (PL) center formed in Cz-Si heated between 450 and 600 °C which has neither been irradiated to produce carbon interstitials, or soaked in hydrogen. It seems that interstitials formed from oxygen precipitates can produce C_i, which reacts with isolated H interstitials possibly produced by the breakup of preexisting molecules, and then diffuses to C_s. There are a number of PL centers produced in this way, and several contain C, O, and H in various proportions.

The plan of this paper is to first review studies of the C_s and C_i defects in Secs. II A and II B. We then briefly discuss hydrogen complexes, especially those that involve intrinsic defects, and in Sec. III we outline our calculational technique. In Sec. IV, we consider two defects involving H bound to substitutional carbon defects, namely C_s-H and C_s-H_2^*. As stated above, the first of these was apparently detected in DLTS studies. Then, in Secs. V A and V B, we discuss the interstitial carbon defects, C_i-H and C_i-H_2. The dicarbon centers C_s-(C_i-H) and C_2-H_2 are described in Secs. V C and V D. Finally, we give our conclusions in Sec. VI.

II. PREVIOUS STUDIES

A. Substitutional carbon

Substitutional carbon defects, C_s, in Si were first detected through infrared spectroscopy by the observation of a local vibrational mode (LVM) at 607 cm^{-1}.[6,7] This frequency is about 80 cm^{-1} above the Raman peak of Si at 523 cm^{-1}, suggesting that a light impurity is involved or else a defect with a strengthened force constant. The presence of carbon

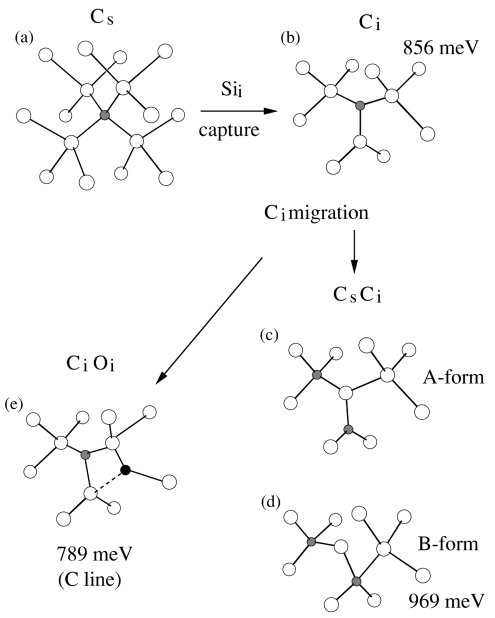

FIG. 1. Low-temperature ($T<300\,^{\circ}$C) carbon-related centers in silicon: (a) The substitutional carbon defect. (b) The isolated interstitial carbon defect. (c) The *A* form of the dicarbon defect. (d) The *B* form of the dicarbon defect. (e) The interstitial carbon-oxygen complex.

was confirmed by the shift in the LVM to 589 and 573 cm^{-1} for ^{13}C and ^{14}C, respectively. No electrical activity has been correlated with the defect, while x-ray studies[8] of carbon-rich Si suggest that the C-Si bonds are significantly shorter than the bulk Si-Si bond. These short C-Si bonds impose an inward, tensile, strain on the lattice hence, causing carbon to act as a sink for interstitial defects which locally compress the lattice. Carbon is also much more electronegative than silicon and the polarization can also attract other impurities. The resulting complexes are often—but not invariably—electronically active, and persist to a higher temperature than the isolated interstitial defect. This trapping can be of use as, for example, Si interstitials are trapped by carbon with the consequent reduction in the unwanted diffusion of boron, whose migration is mediated by silicon interstitials.[9] Oxygen interstitials can also bind to the substitutional defect,[10–12] and form an electrically inactive defect which is stable to 600 °C.

The main properties of substitutional carbon have been confirmed by theory. Previous local-density-functional (LDF) calculations[13,14] found that the inactive substitutional defect, illustrated in Fig. 1(a), remained on site with a C-Si bond length about 10% shorter than that of Si in good agreement with the x-ray measurements.[8] Its vibrational mode is very sensitive to the C-Si bond length, and is calculated to lie between 561 and 684 cm^{-1}, in fair agreement with the experimental value of 607 cm^{-1}. Theory has shown that one oxygen atom is readily trapped by the defect,[15] and it seems that this impurity avoids the very short Si-C bond and bridges an adjacent Si-Si bonds.

B. Interstitial carbon

As discussed above, mobile silicon interstitials are also trapped by C_s, forming the interstitial carbon defect C_i.[16,2] The neutral C_i defect was first detected by infrared absorption experiments on room temperature *e*-irradiated Si,[10] where two high-frequency LVM's at 921 and 930 cm^{-1} were observed. C_i is an electrically active defect with deep donor and acceptor levels, and remarkable in the sense that it is has been observed by all the main characterization techniques.

DLTS studies gave donor and acceptor levels at $E_v+0.28$ and $E_c-0.10$ eV, respectively.[17,18] Electron paramagnetic resonance (EPR) experiments[18,19] show that both charged defects possess C_{2v} symmetry. A large C-related anisotropic hyperfine interaction was found for the C_i^+ defect implying that the donor level was due to a *p* non-bonding orbital on the C radical.[19] In contrast, there was no shift of the hyperfine interaction with carbon isotopes found for C_i^-.[18] This implies that the acceptor wave-function has little amplitude with C. The vibrational modes at 921 and 930 cm^{-1} appear in a 2:1 intensity ratio, suggesting the neutral defect has trigonal symmetry. However, uniaxial stress studies on the two LVM's (Ref. 20) showed that the neutral defect has the same C_{2v} symmetry as both charged defects. C_i also possesses a photoluminescent (PL) line[21] found at 856 meV. This transition is inexplicably unaffected by a change in the C isotope, and there are no phonon replicas which might have revealed the presence of carbon, but the PL has been assigned to the defect, as both it and the infrared-absorption intensities disappear together above room temperature. The bound exciton is believed to be composed of a localized hole trapped in the deep donor level and a delocalized electron. The energy barrier to a reorientation of the defect was determined by EPR (Refs. 19 and 18) to be approximately 0.8 eV—the same as the activation energy deduced from the disappearance of the LVM's. Accordingly, this is taken to be the long-range migration barrier for the defect as it hops between lattice sites.[22]

The microscopic structure proposed for the defect is the same for all three charge states and where C-Si form a split interstitial with a $\langle 100\rangle$ orientation illustrated in Fig. 1(b). Thus both C and the Si atom which share the lattice site have unsaturated bonds.

Theoretical calculations have provided support for the structural model of the interstitial.[23–29] The calculated LVM's (Refs. 24 and 29) are around 900 cm^{-1}, and in reasonable agreement with the observed ones. Theory gives the migration/reorientation energy barriers to be about 0.55–1.10 eV,[25,26,29] again in fair agreement with the experimental results, although there is still controversy over the migration path. However, theory is still unable to determine the precise donor and acceptor levels, although the overall properties of the donor and acceptor wave functions[26,29] are in agreement with those inferred from the EPR measurements.

Above room temperature, the C_i defect becomes mobile, and can complex with other defects and impurities. In low oxygen content material, the C_i-C_s defect is formed when C_i is trapped by C_s. This defect is bistable, existing in two configurations, labeled *A* and *B*, depending on charge state.[30] EPR and DLTS studies showed that the *A* form possessed C_{1h} symmetry and was the stable form for both singly charged defects, $A^{+/-}$, while the *B* form is stable in the neutral charge defect. The defect can be converted into a metastable form by the sudden injection of carriers as in a light pulse or a switch in bias potential. The 0/+ and −/0

levels of the A form lie at $E_v+0.09$ and $E_c-0.17$ eV, respectively. The neutral state refers to the metastable defect. EPR studies showed[30] that the carbon atoms are inequivalent in this configuration, and the g tensor was perturbed by stress in a very similar way to the isolated C_i defect. The model deduced from these experiments consists of a $\langle 100\rangle$-oriented C-Si split-interstitial perturbed by a second carbon atom at a substitutional site, and bonded to the undercoordinated Si atom.[30] Figure 1(c) shows the structural model for the A form of the di-carbon defect.

Optically detected magnetic resonance studies showed that the B form, stable in the neutral charge state, has C_{3v} symmetry for $T>30$ K, and C_{1h} symmetry at lower temperatures.[31] In this form the two C atoms are equivalent. The PL line at 969 meV, associated with the B form, as Zeeman studies shows that the defect is neutral in the ground state, displays carbon-related phonon sidebands at 597.5 and 543.0 cm^{-1}. The isotope shifts of these implied that the modes are dynamically decoupled. The $-/0$ and $0/+$ levels lie at $E_v+0.07$ and $E_c-0.11$ eV, respectively. This time the charged states refer to the metastable B configuration. The barrier between A and B forms is around 0.2 eV. Annealing studies indicate that the dicarbon defect disappears by dissociating around 300 °C. Song *et al.*[30] proposed that a twofold-coordinated Si atom lies between two C_s atoms, as illustrated in Fig. 1(d). Note that there is no C-C bond in the defect.

Recent theoretical calculations[24,29] give support to these models. The A form is found to be more stable than the B form for the $\pm$ charge states, but the neutral A form was still ~ 0.35 eV more stable than the neutral B form, in conflict with experiment.[29] However, the calculations did reveal the presence of two decoupled vibrational modes in the B form each associated with the vibration of a single C atom against its back bonds, and resolving the long-standing problem of the LVM's arising from the PL measurements. The modes arising from the movement of Si_i also involves the motion of both C atoms but their extreme anharmonicity leading to a short lifetime probably prevents their observation.[29]

Other impurities are known to interact with C_i, for example oxygen[2] and phosphorus.[32] Theoretical modelling of the C_i-O defect shown in Fig. 1(e) was given in Ref. 33, while the C_i-O_2 center was discussed in Ref. 34. The stable form of the C_iP_s pair is the same as the isolated C_i defect shown in Fig. 1(b), but the sp^2-bonded Si is replaced by P. This configuration gives rise to donor and acceptor levels at $E_v+0.48$ and $E_c-0.38$ eV, respectively. There are several other metastable forms known.[32]

C. Hydrogen

A wide range of experimental studies have found that hydrogen is also a common contaminant in silicon.[35] It is believed that the molecular form is a common interstitial defect, but its concentration is uncertain as it is inert. In plasma-treated material, Raman-scattering studies[36] show hydrogen modes around 4100 cm^{-1} which have been attributed to molecules close to the surface. Recent reports suggest that the molecule can be trapped near oxygen, and an infrared-active stretch mode lies around 3900 cm^{-1}.[37] There are many indications of the presence of hydrogen even when it is not intentionally introduced. For example, several PL lines found in heat-treated material are also present in Si deliberately doped with H, and these lines are shifted by deuterium,[38–40] demonstrating that H forms part of the defect.

The monatomic neutral defect has been detected by EPR ($AA9$ center) in samples where it is implanted at low temperatures.[41,42] The activation energy for the migration H^+ is 0.43 eV,[41,43,44] and this low value suggests that almost all the H could be trapped at other defects or as molecules. It is believed that the $0/+$ and $-/0$ levels associated with the isolated defect have inverted ordering with the former at $E_c-0.16$ eV and the latter around midgap.

Low temperature proton implantation produces many H defects besides the isolated interstitial. These include (a) VH_n defects with $n\leqslant 4$; (b) the H_2^* defect which consists of a H atom at a bond-centered site adjacent to H at an antibonding site;[45] and (c) the passivated silicon self-interstitial Si_iH_2.[46] With the exception of VH_4, these defects are stable up to $\sim$ 150 °C. The Si_iH_2 defect has a carbon analog which will be considered here.

H forms electrically inactive complexes with many impurities especially shallow donors and acceptors (which are stable until about 250 °C),[47] and transition-metal impurities.[48] Its interaction with carbon will be considered in Sec. II E.

Theoretical calculations[49] suggest that an isolated H interstitial is bistable and diffuses rapidly. In the positive and neutral charge states, H preferentially sits at the bond-centered (BC) site, while in the negative charge state the T_d site is the ground-state configuration.

D. Previous work on C_s-H complexes

Recent DLTS experiments[50–52,4] suggested that hydrogen can be trapped by C_s, forming the $E3$ defect with an $0/+$ level at $E_c-0.15$ eV. The presence of both C and H in the defect was inferred from the variation in the trap concentration with [C] and [H]. It is believed that the defect contains only one C atom and one H atom and does not contain oxygen, although there is no direct evidence for this constitution. The stability appears to depend strongly on charge state. $[C\text{-}H]^+$ anneals out at 80 °C with a rate $\nu e^{-E/kT}$, where the activation energy E is 0.7 eV and $\nu\sim 10^7$ s^{-1}. This value of ν suggests that the dissociation of the defect is controlled by the capture of electrons resulting in a less-stable neutral defect. This is supported by observations[4] that light enhances the dissociation, but only outside a depletion layer where photogenerated electrons can be trapped. These experiments show that the neutral defect anneals out at 20 °C. In p-Si, a hole trap (H1), stable to 100 °C, has been correlated with C and H and this dissociates with E and ν being 1.7 eV and 10^{19} s^{-1}. This last figure seems far too large, and suggests that dissociation is not governed by an Arrhenius behavior. The $-/0$ level is placed at $E_v+0.33$ eV. The similarities in the behavior and their spatial distribution led Kamiura *et al.*[4] to suggest that $E3$ and $H1$ arise from a bond-centered and antibonding configuration of a C_s-H defect, respectively, implying that the defect is bistable.

Before detailing the theoretical modelling of the defect to date, the possible C_s-H configurations are described. The four most obvious configurations are the following: (a) H

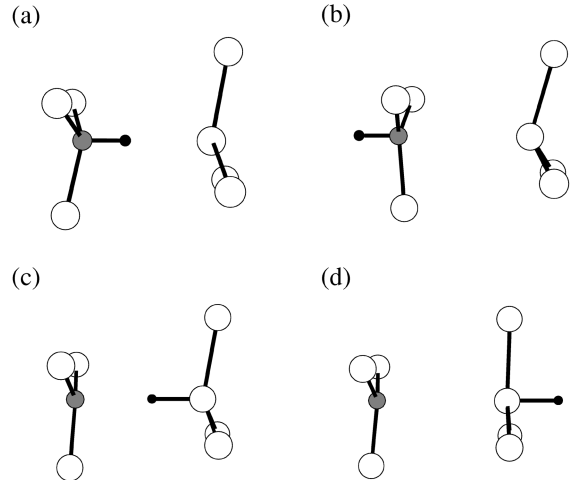

FIG. 2. The possible C_s-H defects in Si: (a) the $(C_sH_{BC})Si$ configuration, (b) the $(H_{AB}C_s)Si$ configuration, (c) the $C_s(H_{BC}Si)$ configuration, and (d) the $C_s(SiH_{AB})$ configuration.

lying near a bond center between C and a Si neighbor but bonded to C. We shall refer to this configuration as $(C_sH_{BC})Si$. (b) H antibonded to C $(H_{AB}C_s)Si$. (c) H bond centered between C and Si but bonded to Si $C_s(H_{BC}Si)$. (d) H antibonded to Si $C_s(SiH_{AB})$. These are illustrated in Figs. 2(a)–2(d). Two further configurations are considered which are related to (b) and (d), but the H atom lies at a T_d site and the C-Si bond is reformed.

Early theoretical modelling of the defect,[53] using Hartree-Fock theory, concluded that there two almost degenerate neutral ground-state configurations. These correspond to structures $C_s(H_{BC}Si)$ and $(H_{AB}C_s)Si$, with the latter being slightly higher in energy (0.05 eV). The binding energy of H to C in this defect was found to be 1.42 eV, and both of these configurations gave rise to defect-related states in the band gap. The $C_s(SiH_{AB})$ configuration was found to be 0.94 eV above the ground state, with the tetrahedral sites being even higher in energy.

More recent calculations on the neutral defect[15] using LDF theory found $(C_sH_{BC})Si$ to be the ground-state energy configuration, in contradiction with the previous calculation. The discrepancy between the two calculations was resolved after further work[54] using standard and post-Hartree Fock techniques on molecular clusters, as well as density-functional-theory calculations in clusters and supercells. The two bond-centered structures $(C_sH_{BC})Si$ and $C_s(H_{BC}Si)$ were found to be the lowest-energy configurations, with LDF calculations predicting $(C_sH_{BC})Si$ as the lowest-energy configuration in agreement with Ref. 15. When Hartree-Fock correlation corrections were included, the lowest-energy configuration switched from $C_s(H_{BC}Si)$ to $(C_sH_{BC})Si$, but the energy difference between these two forms was found to be only a few meV.

In the light of the experimental data which suggests that the ground-state structure changes with charge state, LDF calculations were performed on the C_s-H defect in the three charge states utilizing nine-atom supercells.[55] The stable structure was $(C_sH_{BC})Si$, in all charge states with a H-binding energy of 1.20 eV for the neutral one. In the negative charge state, however, the dissociated configuration where H lies at a tetrahedral T_d site to one of the Si neighbors of C has an energy within 0.06 eV of the ground state. The closeness of these energies suggests that the negatively charged defect is barely stable. The calculations for the relative energies of the metastable neutral structures differed from the previous results. The lowest-energy metastable configuration was $C_s(SiH_{AB})$, lying 0.57 eV above the ground state. Almost degenerate in energy with this structure was $(H_{AB}C_s)Si$, which was 0.61 eV above the ground state.

These results therefore indicated that trapping of two electrons by $(C_s\text{-}H)^+$ could lead to a rapid dissociation and such a change would explain the loss of the $E_c-0.15$ eV state after illumination. For clarity, the main results are summarized, along with the results of our calculations described below in Table I.

E. Previous work on C_i-H related complexes

Minaev and Mudyri[56] observed several sharp PL lines from Cz-Si annealed between 450 and 600 °C. The presence of oxygen and carbon in many of these was deduced from their presence in the material. Deliberate introduction of H and C, followed by *e* or *n* irradiation, can dramatically affect the intensities of some of these PL lines. Isotopic analysis leads to shifts in the lines showing that many of these defects contain carbon (e.g., the *P* and *H* centers) and both carbon and hydrogen (*I*, *M*, and *T* centers).[57,38,58,39,40] The *I*, *M*, and *T* lines are believed to contain one hydrogen atom, due to the splitting of their zero-phonon lines into doublets when both H and D are present in the material.[40]

Of particular interest here is the the *T* line (935.1 meV) which has been studied most extensively. Isotope shifts in this zero-phonon line with ^{13}C (Ref. 57) confirmed the presence of carbon in the defect, and further studies[58] showed that the defect contained H and possessed C_{1h} symmetry. There is no evidence from the splitting of the zero-phonon line in mixed isotopic cases, for more than one C or H atom.

TABLE I. Relative energies (eV) for the C_s-H defect in Si with varying charge state. NF indicates that the structure was not found as a stable or metastable configuration.

	Previous work [a]			Present work		
Structure	+	0	−	+	0	−
$(C_sH_{BC})Si$	0.00	0.00	0.00	0.00	0.00	0.04
$(H_{AB}C_s)Si$	0.70	0.60	0.30	0.49	0.33	0.00
$C_s(H_{BC}Si)$	NF	NF	NF	NF	NF	NF
$C_s(SiH_{AB})$	0.71	0.57	0.06	1.97	1.12	0.79

[a]Reference 15.

However, C-isotopic shifts of an LVM, observed as a phonon replica to the *T* line, demonstrated that the defect contained two C atoms. In recent work,[5] this and other LVM's, along with their isotope shifts, have been detailed, and these results, in conjunction with *ab initio* calculations, have elucidated the microscopic structure of the defect. This consists of a $\langle 100 \rangle$-oriented C-CH pair occupying a single lattice site, the structural model is discussed in more detail in Sec. V. This defect is isoelectronic with C_i-P_s and is also the first C-related defect known to contain a C-C bond and should be contrasted with the dicarbon center discussed above. If the H concentration is large, with respect to C, the *T* line disappears. We shall discuss possible reasons for this in Sec. VI.

The high mobility and reactivity of C_i-H defects suggests that complexes could be formed with many other impurities and recently we have considered a shallow donor defect formed from a complex of C_i-H with pair of oxygen atoms.[59] At the moment there is no definitive evidence that such complexes exist, but there are indications. A shallow H donor called *NL*10(H) has H lying along a [110] axis is stable to 520 °C.[60] This seems a distinct defect from the H-passivated thermal donors[61] which are stable up to 200 °C. However, there is no evidence for the involvement of carbon at the present time.

III. METHOD

We carry out LDF cluster calculations on large hydrogen terminated clusters using the *Ab Initio* Modeling Program (AIMPRO).[62] For most calculations C and H atoms were added to an 86 atom trigonal cluster, $Si_{44}H_{42}$, representing the perfect material. A central Si atom was replaced by C and another H atom added to model the C_s-H defect. In a similar way additional atoms were added to investigate interstitial carbon-hydrogen defects. To explore dissociation and reorientation energies, C and H atoms were added to a larger 131-atom cluster $Si_{71}H_{60}$ cluster representing perfect material.

Norm-conserving pseudopotentials for carbon and silicon were taken from Ref. 63, whereas the full Coulombic potential was used for the H atom. The electronic wave functions were expanded using a basis of *s* and *p* Gaussian orbitals centered on the nuclei, and at the center of selected bonds. Eight Gaussian orbitals of different exponents were used on the C atom(s), and the innermost Si atoms. A fixed linear combination of eight Gaussians was used on all other Si atoms. Three Gaussian orbitals with different exponents were sited on the defect-related H atoms, and a linear combination of these Gaussian orbitals were used for the terminating H atoms. Additionally, three *s* and *p* Gaussian orbitals with different exponents were placed at the center of every bond in and around the defect core. The charge density was expanded in a basis of *s* Gaussian functions sited at the same sites as above with the same number of different exponents. The self-consistent energy and the forces on each atom were then calculated, and the structure relaxed by a conjugate gradient algorithm until the energy minima was found.

In order to calculate the dynamical matrix, the second derivatives of the energy with respect to atomic position were calculated for the C atoms, along with the neighboring silicon atoms, and defect H atoms. A Musgrave-Pople potential found previously[64] was used to construct the remaining entries in the dynamical matrix for the cluster. From this, the vibrational frequencies of the cluster, and their normal coordinates were found. Further details are given in Ref. 62.

The procedure for determining the migration barrier for the defects investigated here is as follows: The saddle point for the possible migration paths are not clear for the defects investigated in this work, so to estimate it the following procedure was taken: Vector displacements of equivalent atoms from two low-energy configurations were determined, $\mathbf{v}_i = \mathbf{R}_i^1 - \mathbf{R}_i^2$, where $\mathbf{R}_i^1$ and $\mathbf{R}_i^2$ refer to the staring and ending atomic configurations. All atoms were then moved along the vector $\mathbf{v}_i$ by a fraction α to give the intermediate points in the migration, and then all atoms were allowed to relax from these positions subject to a further constraint that the vector of further displacements are perpendicular to $\mathbf{v}_i$, until the optimization was complete. The result of this is a profile of the energy as a function of α for the restructuring of the defect, and the barrier for migration and/or reorientation corresponds to the maximum value of energy obtained, at the corresponding saddle configuration.

Typically, variations of up to 0.3 eV in the relative energies of configurations were found, as the energy converged with increasing cluster size. For the defects investigated here, in which the difference in ground-state energies was small, and any variations may critically affect the migration barriers (namely, C_iH), calculations performed on a number of larger clusters confirmed that the energy had converged with the results being independent of cluster size.

IV. SUBSTITUTIONAL CARBON-HYDROGEN COMPLEXES

A. C_s-H defect

The C and H atoms were introduced into the center of the 86-atom cluster with atomic positions and bond lengths chosen to form all four possible structures outlined in Sec. II, Figs. 2(a)–2(d). All atoms were then allowed to relax with the symmetry constrained to C_{3v}. Table I shows the relative energies of the various configurations. In agreement with all recent theoretical calculations, (C_sH_{BC})Si was found to be the most stable structure in the neutral charge state. Our trends in energies against charge state are in agreement with those of Ref. 55, although we disagree on the metastable structures. These trends are illustrated in Fig. 3, and are given along with the results of the previous calculation in Table I. The energy differences between the stable and metastable configurations decrease as the charge state changes from positive to negative in both the present results, and the previous calculation.

The defect is bistable with H lying at a BC site but bonded with C, the (C_sH_{BC})Si configuration, Fig. 2(a), being the most stable one in the neutral and positive charge states. In the negative charge state however, the configuration where H lies at an AB site while still bonded with C, i.e., $(H_{AB}C_s)$Si, in Fig. 2(b) is the most stable.

For all charge states, $C_s(H_{BC}Si)$ is unstable and H moves spontaneously along $\langle 111 \rangle$, bonding with C to form the (C_sH_{BC})Si structure, Fig 2(a). This agrees with the results of Ref. 15, but is in disagreement with the results of Refs. 53 and 54, when it was found that $C_s(H_{BC}Si)$ was metastable.

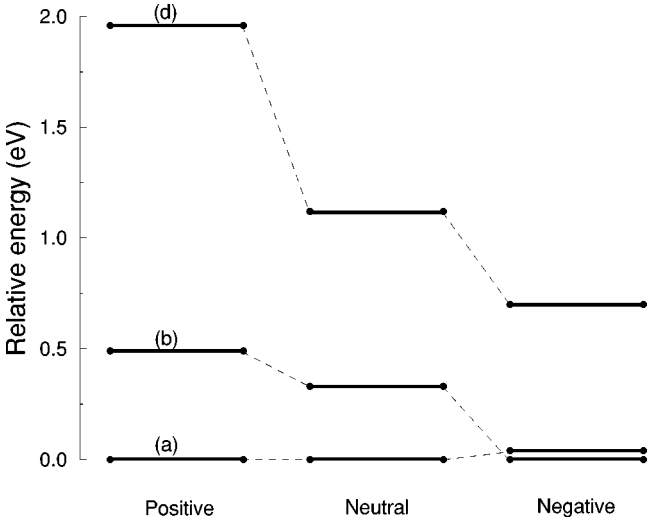

FIG. 3. Trends in relative energies of the various configurations of the C_s-H defects with varying charge state.

Kaneta and Katayama-Yoshida[15] found that the $C_s(SiH_{AB})$ in the negative charge state to be almost degenerate with $(C_sH_{BC})Si$, but we found a difference of energies of 0.75 eV.

The optimized bond lengths for the three stable structures and their variation in charge state are given in Table II. These results show that H moves almost to the the T_d site in the negative charge state of $C_s(SiH_{AB})$. This was the only tetrahedral configuration found. Our result is in disagreement with the previous study,[55] where it was found that the tetrahedral defect formed in the negative charge state, similar to isolated hydrogen.

We now consider the energy levels of the different structures in the neutral charge state. All three stable configurations gave rise to a deep level which is singly occupied as shown in Fig. 4. Here the Kohn-Sham eigenvalues are scaled to the band gap of silicon. The theory is not able to predict accurately the donor/acceptor levels but it is clear from the Kohn-Sham eigenvalues that in all cases when H complexes with C_s an electrically active defect remains. These results are consistent with the tentative assignment of $E3$ and $H1$ to the $(C_sH_{BC})Si$ and $(H_{AC}C_s)Si$ structures, respectively.[4]

The binding energy of neutral H with C_s is found to be 1.01 eV by comparing the energies of the complex with its dissociated constituents using a 132-atom cluster. In the dissociated form a neutral H lies at a BC site remote from C_s. This low binding energy is similar to those found in previous calculations. This suggests that H released by a break up of molecules or platelets can be trapped by C_s.

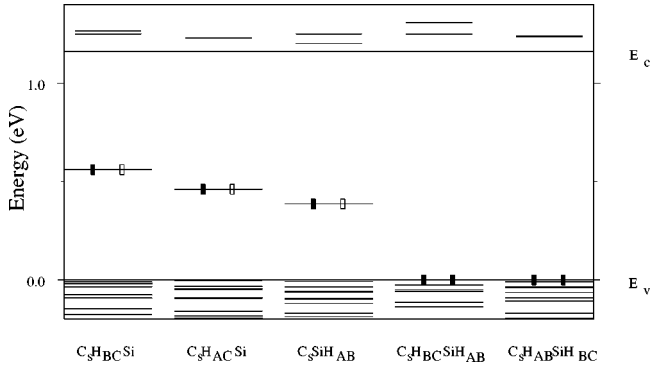

FIG. 4. The Kohn-Sham levels of the substitutional carbon-hydrogen defects.

B. C_s-H_2 defect

The unstable nature of C_s-H as demonstrated by its low dissociation energy suggests that it readily complexes with other impurities and especially a second H atom. One possibility is that a H_2 molecule would be formed and this might lie close to C_s attracted by the polarization field. A second possibility is that a H_2^* defect bound to carbon is formed. Since the defect contains CH bonds, it is expected to be more stable than a solitary H_2^* defect which disappears at 200 °C.[45]

There are two likely structures for this defect: (a) the $(C_sH_{BC})Si$ structure of C_s-H, with the second hydrogen at the anti-bonding silicon site, and (b) the $(H_{AB}C_s)Si$ configuration with the second hydrogen bonded to Si, and at the bond-centered site. These are labeled $(C_sH_{BC})(SiH_{AB})$ and $(H_{AC}C_s)(H_{BC}Si)$, respectively, and are illustrated in Figs. 5(a) and 5(b). Their total energies are almost identical, the first configuration being lower in energy by 0.02 eV. Details of their structure are given in in Table III. The Kohn-Sham eigenvalues are illustrated in Fig. 5, and show that the defects are electrically inactive. The LVM's for both configurations have been calculated, and are given, along with their symmetries, in Table IV. There have been no reports of these modes, to our knowledge. The highest modes of each configuration correspond to C-H and Si-H stretch, respectively. It is likely that these modes are overestimated by about 10% as similar calculations give this overestimate for both VH_n defects in Si (Ref. 65) and C-H defects in GaAs.[66] The compressed Si-H bond in the second configuration results in a significant increase of its stretch mode compared to that of the first. The C-H and Si-H wag modes are much higher than those in the second configuration. Both configurations give rise to a carbon related E mode around 650 cm^{-1}. The large differences in the wag and stretch modes of these C_s-H_2

TABLE II. Bond lengths of the three stable configurations of C_s-H in Si, in Å.

	$(C_sH_{BC})Si$			$(H_{AB}C_s)Si$			$C_s(SiH_{AB})$		
Charge state	+	0	−	+	0	−	+	0	−
C-H	1.093	1.096	1.102	1.082	1.084	1.086	3.724	5.234	4.953
Si-H	2.214	2.190	2.109	4.826	4.655	4.439	1.610	1.507	1.518
C-Si	3.307	3.287	3.211	3.744	3.571	3.353	2.114	3.727	3.435
C-Si (3)	1.987	1.968	1.941	1.992	1.979	1.963	1.989	1.891	1.863

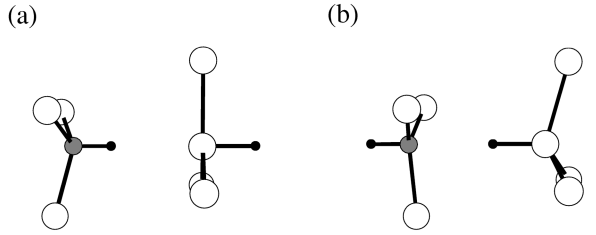

FIG. 5. The C_s-H_2 configurations investigated: (a) the $(C_sH_{BC})(SiH_{AB})$ configuration, and (b) the $(H_{AC}C_s)(H_{BC}Si)$ con-

defects suggests that their measurement might enable the models of the defect to be distinguished.

V. INTERSTITIAL CARBON-HYDROGEN DEFECTS

A. C_i-H defect

The isolated C_i defect shown in Fig. 1(b) possesses two undercoordinated atoms (C and Si), and therefore H could readily bond to either of these atoms forming a $\langle 100\rangle$-oriented defect with H bonded to C, Fig. 6(a), or with H bonded to Si (not illustrated). These configurations are labeled $(C_iH)_{\langle 100\rangle}Si$ and $C_i(SiH)_{\langle 100\rangle}$. There is also the possibility of a structural change to a BC form with either the C-H unit at the center of a Si-Si bond $(C_iH)_{BC}Si$, Fig. 6(b), or with a Si-H unit at the center of a C_s-Si bond $C_s(Si_iH)_{BC}$. All four of these configurations possess C_{1h} symmetry.

The four configurations were inserted into a tetrahedral 131-atom cluster, and all atoms were relaxed. The defects retained their C_{1h} symmetry throughout the relaxation. The resulting energies and structural details of the four configurations are given in Tables V and VI. Two structures possessed almost degenerate energies in the neutral charge state: the BC defect described as $(C_iH)_{BC}Si$ possessed a energy 0.03 eV above the $(C_iH)_{\langle 100\rangle}Si$ structure. The other structures were less stable by at least 0.47 eV. The binding energy of H with C_i in the [100] form was evaluated in the same way as described above for C_s-H. This gave a value of 2.8 eV which is, as expected, considerably greater than the binding of H with C_s.

The near degeneracy in the energies of the [100] and BC forms is surprising in view of the very different bonding patterns. These two configurations possessed very different energies for the C_i defect, and it is the presence of H which stabilizes the BC form. The results suggest that the defect could rapidly diffuse. This is because a long-range diffusion path can be constructed connecting these forms. The saddle point for this migration path was found by the following procedure. A number of constrained relaxations were carried out as described in Sec. III. The initial cluster coordinates in each run were linearly interpolated between the relaxed $\langle 100\rangle$ and $\langle 111\rangle$ bond-centered forms illustrated in Figs. 6(a) and 6(b). Thus these coordinates are simply $(1-\alpha)R_1 + \alpha R_2$, where R_i describes the $\langle 100\rangle$ and $\langle 111\rangle$ forms, respectively. At each point along the line joining the configurations, the cluster was fully relaxed, with the constraint that the component of the force on each atom along this direction was set to zero. The energies of each run versus α are shown in Fig. 7 (α_1). As the defect moves away from the $\langle 100\rangle$ configuration into the $\langle 111\rangle$ BC form, the energy rises until

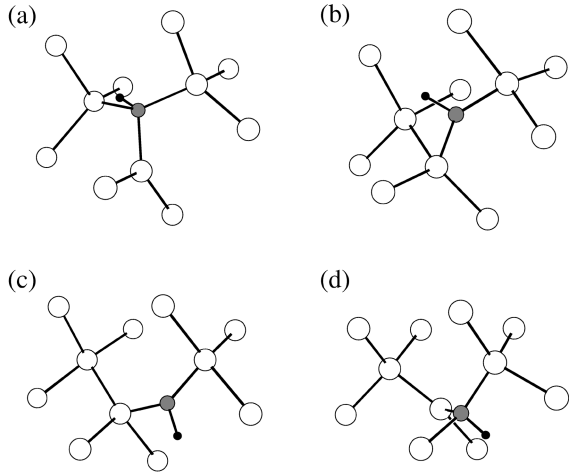

FIG. 6. The possible configurations of the C_i-H defect in Si, and the defect migration path: (a) the $(C_iH)_{\langle 100\rangle}Si$ configuration, (b) the $(C_iH)_{BC}Si$ configuration, (c) the $(C_iH)_{BC}Si$ configuration with the rotated CH unit, and (d) reformation of the $(C_iH)_{\langle 100\rangle}Si$ structure.

~ 0.27-eV peaking around $\alpha = 0.6$, and then dropping as the BC form is realized. This value of α corresponds to the barrier for interconversion between the two low-energy forms of the defect. There is then the possibility of a $\pm 120°$ rotation of the bond-centered C_i-H unit about the $\langle 111\rangle$ axis, the BC defect having three equivalent structures. A second constrained run with R_i representing the BC_1 and BC_2 configurations, Figs. 6(b) and 6(c), was performed, and the results are shown in Fig. 7 (α_2). The 0.16-eV barrier for the rotation of the bond-centered CH unit is lower than the barrier for interconversion between the two different structures, and peaks around $\alpha = 0.25$ and 0.75. There is a slight reduction in energy at $\alpha = 0.5$ to 0.11 eV, where the C_i-H unit passes through a C_{1h} mirror plane (corresponding to a rotation through 60°). Following the rotation of the BC defect, the migration process is completed with the reformation of the $\langle 100\rangle$-oriented defect, Fig. 6(d).

From these results, it is clear that the migration energy for this defect is extremely low, around 0.3 eV. This is consid-

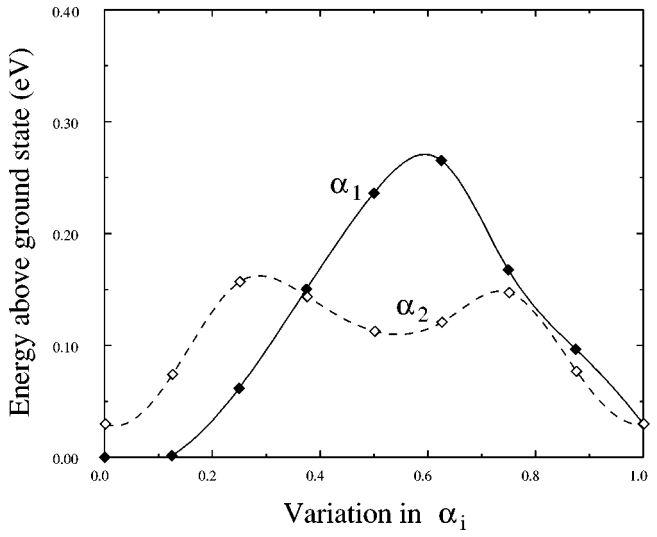

FIG. 7. The energy as a function of α for the restructuring and rotation of the C_i-H defect.

TABLE III. Bond lengths of the two possible configurations of C_s-H_2 in Si, in Å.

	$(C_sH_{BC})(SiH_{AB})$	$(H_{AC}C_s)(H_{BC}Si)$
Charge state	0	0
C-H	1.097	1.084
Si-H	1.501	1.484
C-Si (3)	1.976	1.984
Si-Si (3)	2.324	2.312

erably lower than the 1.1 eV calculated for the migration of C_i,[29] where the observed value is 0.8 eV. It may seem surprising that the C_i-H defect diffuses easier than C_i. However, we think this reflects the low energy of the BC configuration which is stabilized by the H atom: without H, the C atom would possess two dangling bonds. We therefore expect the C_i-H defect to be an extremely reactive unit, rapidly migrating to and complexing with other defects present in the material.

The defect gives rise to a gap level which contains one electron. For $(C_iH)_{\langle 100\rangle}Si$, this was above midgap, and the level appeared below midgap for the $(C_iH)_{BC}Si$ structure. Although we cannot exactly place the defect levels accurately, it is clear that this positioning of these levels is consistent with the highest occupied state being a single electron occupying either a Si- or C-related p orbital. Hence the defects are paramagnetic in the neutral charge state with $S=\frac{1}{2}$. The Kohn-Sham levels for all four of these configurations, as well as their dependence on the charge state, are illustrated in Fig. 8.

We now investigate the charged C_i-H defects. Their structures are almost identical to the neutral defect. Table V shows the energies of the charged configurations. It is clear that the difference in energy between the two forms of the charged defect is much greater than the neutral case. In the negative charge state, the BC structure proved to be lowest in energy—being 0.55 eV below the $\langle 100\rangle$ structure. Conversely, in the positive charge state the $\langle 100\rangle$-oriented defect lays 0.72 eV below the BC configuration. The greater difference in the energies of the two forms must result in a greater diffusion energy for the charged defects, and these must be at least 0.55 and 0.72 eV, respectively, if the same paths are followed. These are comparable with the migration energy for C_i.

The LVM's are given in Table VII for the neutral defect. Anharmonic effects will probably be considerable as the highest modes, and, as the energies for these excitations are close to the migration energy of the neutral defect, they are unlikely to be detected. This is similar to the situation for the dicarbon defect.[29]

B. C_i-H_2 defect

The rapid diffusivity of C_i-H suggests that it is likely to easily react with other impurities, and we now consider the effects of the addition of a second H which would render the defect electrically inactive and probably immobile. Once again, there are two likely configurations for the C_i-H_2 defect arising from the saturation of the radical in C_i-H: the $\langle 100\rangle$-oriented CH-SiH split interstitial, Fig. 9(a) labeled $(C_iH_2)_{\langle 100\rangle}$ and a $(C_i$-$H_2)$ unit lying at a bond center between two silicon atoms [Fig. 9(b)], $(C_iH_2)_{BC}$. The first of these does not possess any symmetry, and the latter has C_{1h} symmetry.

An 88-atom cluster $CSi_{43}H_{44}$ was used to investigate these forms. The BC structure proved to be lowest in energy, being 0.58 eV below the $\langle 100\rangle$ structure. This reflects the strong C-H bond strength. Figure 7 shows that the second H has completely passivated the defect. Table VI gives its structural data, and its vibrational modes are given in Table VIII.

TABLE IV. Calculated local vibrational modes of the two C_s-H_2 configurations along with their isotope shifts.

Symmetry	^{12}C H H	^{12}C {H,D} mix	^{12}C D D	^{13}C H H
$(C_sH_{BC})(SiH_{AB})$				
A_1	3004.3	3004.3 2204.3	2203.6	2995.7
A_1	2135.1	1532.3 2134.4	1532.3	2135.1
E	1232.1	1232.1 925.0	915.3	1228.6
E	920.0	655.1 911.0	654.6	920.0
E	642.3	641.2 617.4	617.4	627.0
$(H_{AC}C_s)(H_{BC}Si)$				
A_1	3053.2	3051.5 2420.8	2234.4	3045.1
A_1	2412.3	1732.4 2227.1	1731.9	2412.3
E	1074.8	1074.7 791.4	791.2	1073.1
E	664.8	664.3 641.5	641.1	648.9
E	629.1	429.1 629.0	429.1	628.7

TABLE V. Relative energies for the C_{in}-H_m structures examined in this work.

Configuration	Description	Relative energy (eV)
C_i-H		
$(C_iH)_{\langle 100\rangle}Si$	A $\langle 100\rangle$-oriented C-Si split interstitial with a C-H bond $(0,+,-)$	0.00, 0.00, 0.55
$C_i(SiH)_{\langle 100\rangle}$	A $\langle 100\rangle$-oriented C-Si split interstitial with a Si-H bond	0.47
$(C_iH)_{BC}Si$	A bond-centered C_i-H defect $(0,+,-)$	0.03, 0.72, 0.00
$C_s(Si_iH)_{BC}$	A bond-centered Si_i-H defect with a neighboring C_s	1.65
C_i-H_2		
$(C_iH_2)_{\langle 100\rangle}$	A fully passivated $\langle 100\rangle$-oriented C-Si pair	0.58
$(C_iH_2)_{BC}$	A bond-centered C_i-H_2 defect	0.00
C_s-(C_i-H)		
A-C_sC_iH	The A form of C_i-C_s with H bonded to the C_i	0.55
B-C_sC_iH	The B form of C_i-C_s with H bonded to the Si_i	1.81
$C_s(C_iH)_{BC}$	The C-H BC model with the Si labeled 1 and 2 [Fig. 10(b)] replaced by C	0.28
$C_s+(C_iH)_{BC}$	The C-H BC model with the Si labeled 3 and 4 [Fig. 10(b)] replaced by C	0.68
$C_s(C_iH)_{\langle 100\rangle}$	A $\langle 100\rangle$ C-CH split interstitial with H lowering the symmetry to C_{1ht}	0.00
C_2-H_2		
$(C_2H_2)_{\langle 100\rangle}$	A $\langle 100\rangle$-oriented C_2-H_2 defect	0.00
$(C_2H_2)_{BC}$	A bond-centered C_i-H_2 defect with a neighboring C_s	0.99
$(C_2H_2)_{\langle 110\rangle}$	A $\langle 110\rangle$-oriented C_2-H_2 defect	3.59

Since this defect is electrically inert and possesses high thermal stability, it is surprising that there have been no reports of its associated vibrational modes. Its Si_iH_2 analog has been detected in low-temperature proton-implanted samples,[46] and has been the subject of theoretical calculations.[67,68,46]

C. C_s-(C_i-H) defect

Another possible reaction which C_i-H might undergo is trapping by C_s. As well as by capture of C_iH by C_s, a C_s-(C_i-H) defect could be formed by the capture of H by the dicarbon defect. These structures will also be investigated, and, in Sec. V D, we will outline the most likely formation mechanism of all of these defects.

There are of course many possible configurations of such defects but the most likely ones are the following: (a) The A form of the dicarbon defect with H bonded to either of the undercoordinated atoms. (b) The B form of the dicarbon defect with H bonded to the Si_i. (c) A $\langle 100\rangle$-oriented C-(CH) interstitial defect with these atoms occupying a single lattice site [Fig. 10(a), labeled $C_s(C_iH)_{\langle 100\rangle}$]. (d) A bond-centered C_i-H unit with a neighboring C_s atom [Fig. 10(b), sites 1 and 2, labeled $C_s(C_iH)_{BC}$]. (e) A bond-centered C_i-H unit with a substitutional carbon atom in the next nearest neighbor site

TABLE VI. Calculated bond lengths for the interstitial carbon-hydrogen complexes investigated in this work. Subscripts refer to the atoms coordination and numbers in brackets indicate the multiplicity of the bonds.

Structure	Bond				
$(C_iH)_{\langle 100\rangle}Si$	C_4-H	C_4-Si_4	C_4-Si_3	Si_3-Si_4	
	1.092	1.944 (2)	1.861	2.249, 2.252	
$(C_iH)_{BC}Si$	C_3-H	C_3-Si			
	1.078	1.797, 1.811			
$(C_iH_2)_{BC}$	C_4-H	C_4-Si			
	1.090	1.860, 1.872			
$C_s(C_iH)_{\langle 100\rangle}$	C_4-H	C_4-Si_4	C_4-C_3	C_3-Si	
	1.107	2.047 (2)	1.460	1.908	1.914
$C_s(C_iH)_{BC}$	C_3-H	C_3-C_4	C_3-Si	C_4-Si	
	1.115	1.404	1.816	2.126, 2.184 (2)	
$(C_2H_2)_{\langle 100\rangle}$	C-H	C-C	C-Si		
	1.085	1.500	2.014	2.019	

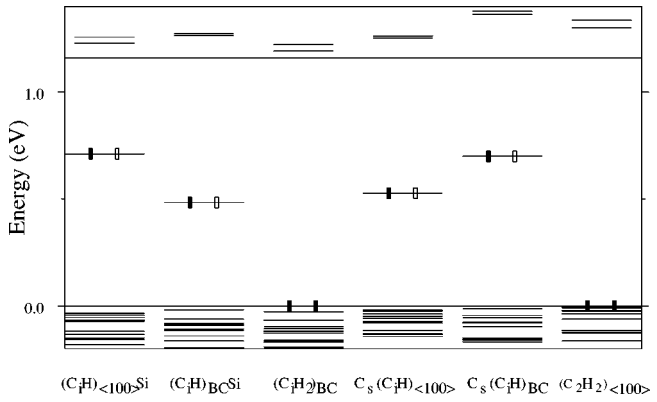

FIG. 8. The Kohn-Sham levels of the interstitial carbon-hydrogen defects.

TABLE VII. Calculated local modes of C_i-H configurations, cm^{-1}.

Symmetry	^{12}CH	^{12}CD	^{13}CH
$(C_iH)_{BC}Si$			
A	3050.0	2234.6	3041.6
A	1142.8	772.0	1134.7
A	952.4	1010.1	928.1
B	627.8	549.8	622.0
A	573.7	569.6	569.4
$(C_iH)_{\langle 100\rangle}Si$			
A	3029.2	2219.5	3020.8
B	1038.0	797.9	1035.2
A	974.3	786.5	969.3
A	727.1	649.9	710.0
B	683.6	652.7	664.7

[Fig. 10(b), sites 3 and 4]. (f) A ⟨110⟩-oriented split-interstitial defect with the C-CH occupying a single lattice site. All of the above configurations possessed C_{1h} symmetry.

The defects were inserted into 86-atom clusters, and all atoms relaxed with a full symmetry constraint until the equilibrium geometries were determined. The ground-state configuration consists of (c), where H saturates a C radical in the ⟨100⟩-oriented C-C split interstitial. The relative energies of the other configurations are listed in Table V. A second configuration $C_s(C_iH)_{BC}$ has an energy 0.28 eV higher. It is interesting to note that both low-energy configurations possess a C-C bond, contrary to the case for the isolated dicarbon center. The neutral ground-state structure is paramagnetic, with $S=\frac{1}{2}$, and is isoelectronic with the *IA* configuration of the C_i-P_s defect which was investigated experimentally.

The Kohn-Sham eigenvalues are shown in Fig. 7, and indicate that the defect gives rise to one gap level, containing one electron. This occurs around midgap, and is related to a nonbonding *p* orbital on the undercoordinated carbon atom. An estimate for the donor and acceptor level positions was obtained using the Slater transition method, and scaling the results to the experimental band gap. This gave the acceptor level at $E_c-0.39$ eV, in reasonable agreement with the observed value of $E_c-0.20$ eV. The donor level was found to be at $E_v+0.28$ eV, and as thus far escaped detection experimentally.

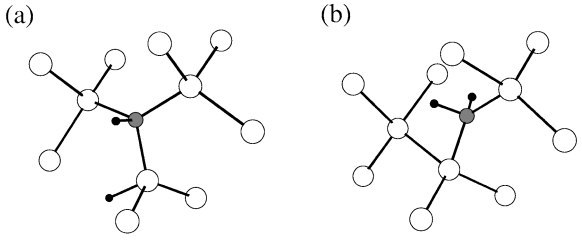

FIG. 9. The possible C_i-H_2 configurations: (a) the $(C_iH_2)_{\langle 100\rangle}$ configuration, and (b) the $(C_iH_2)_{BC}$ configuration.

TABLE VIII. Calculated local modes of the $(C_iH_2)_{BC}$ configuration, cm^{-1}.

Symmetry	^{12}CHH	^{12}CHD	^{12}CDD	^{13}CHH
A	3092.5	3076.4	2266.9	3087.4
B	3062.5	2252.3	2235.3	3051.4
A	1448.0	1288.9	1066.3	1443.8
B	1121.4	754.6	798.6	1121.4
A	1093.3	1088.8	728.1	1085.8
A	850.6	904.1	923.1	827.9
B	692.6	634.7	601.9	683.3
A	576.0	570.4	567.7	570.5

The defect has been assigned to the 0.9351-eV PL center, or *T* center. The structure and vibrational modes of the ground state structure are given in Table IX and their relationship with the modes observed for the *T* center has been described previously.[5] Analysis of the Zeeman splitting of the PL line confirms that the neutral state of the *T*-line defect is paramagnetic with $S=\frac{1}{2}$ consistent with the singly occupied Kohn-Sham level from the calculation, illustrated along with the BC configuration levels in Fig. 7.

Configuration (d) is a dissociated form of the defect where the C_s and C_i-H units are separated by one silicon atom. The energy of this configuration suggests that the binding energy of C_i-H with C_s is ~ 0.6 eV. Thus the *T* center is a thermally stable defect with an undercoordinated C atom, and may trap a second H atom. This passivated dicarbon center will be discussed in Sec. V D.

D. C_2-H_2 defect

In samples with large concentrations of H, the intensity of the *T* line is greatly reduced. One possible explanation is that the C_i-H precursor defect traps a second H atom, becoming immobile, thus blocking the formation of the *T* center. A second possibility is that the *T* center rapidly traps a second H atom.

Here we investigated three possible configurations of the C_2-H_2 defect, using a 134-atom tetrahedral cluster $C_2Si_{70}H_{62}$, in which all atoms were relaxed. The configurations examined were (a) the ⟨100⟩-oriented defect labeled $(C_2H_2)_{\langle 100\rangle}$; (b) a BC defect, with a C_i-H_2 unit between C_s and a Si neighbor, labeled $(C_2H_2)_{BC}$; and finally (c) $(C_2H_2)_{\langle 110\rangle}$, where two (C-H) units share a lattice site this orientation. The symmetry of these three configurations was constrained to C_2, C_{1h}, and C_{2v}, respectively. The relaxed structures of these defects are illustrated in Figs. 11(a)–

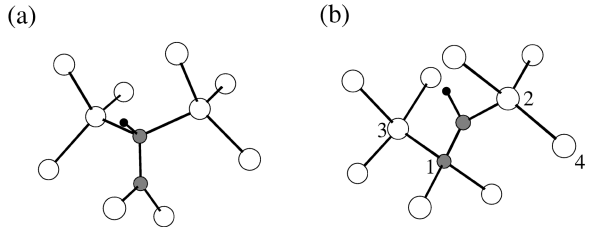

FIG. 10. The low-energy C_2-H defect configurations: (a) the $C_s(C_iH)_{\langle 100\rangle}$ configuration (T-center defect), and (b) the $C_s(C_iH)_{BC}$ configuration.

TABLE IX. Calculated vibrational modes, cm^{-1}, and their downward shifts with C isotopes, of the $\langle 100\rangle$-oriented C-(^{12}C-H) defect, along with those observed form the *T* line.

Symmetry	Mode	^{12}C-(^{12}C-H)	12,13	13,12	13,13	^{12}C-(^{12}C-D)	12,13	13,12	13,13
Calculated									
A		2913.6	8.3	0.0	8.3	2138.3	12.1	0.0	12.2
A		1180.4	1.8	5.5	6.9	892.6	4.5	8.1	12.5
A	*L*5	1097.8	19.2	20.7	40.8	1102.2	17.1	24.3	42.3
B		870.7	1.7	0.0	1.7	643.6	4.0	0.2	4.2
A	*L*4	743.6	1.0	22.0	23.1	713.7	0.9	16.6	17.3
A	*L*3	558.0	4.9	3.4	7.6	552.7	4.0	2.7	6.1
A	*L*2	542.4	3.7	0.2	3.8	539.2	2.5	0.1	2.5
Experiment [a]				Mixed				Mixed	
A	*L*5	1056.0		18.0, 27.0	45.0	1052.0		16.5, 20.5	38.0
A	*L*4	796.0			25.0	759.0			16.5
A	*L*3	567.5		3.0, 7.5	10.0	558.5		2.5, 5.3	7.7
A	*L*2	531.5		2.0, 4.0	5.5	528.0		−1.8, 1.3	2.3

[a]Reference 5.

11(c). The most stable defect is $(C_2H_2)_{\langle 100\rangle}$, where H saturates the C radical in the *T* center. Table V gives the relative energies of the other structures. The Kohn-Sham eigenvalues indicated that the stable defect is electrically inactive. Table VI give its structural details and the LVM's are given in Table X.

The defect is analogous with the hydrogenated self-interstitial defect (Si_iH_2) which also has a $\langle 100\rangle$ orientation[68,46] with C_2 symmetry. For comparison, the calculated and experimentally observed modes for this defect are also given. The C_2-H_2 defect possesses many localized modes lying above the Raman frequency. In addition to C-H stretch and wag modes around 3000 and 1200 cm^{-1}, there is a high-frequency C-C mode at 1040 cm^{-1} as well as local modes from the C-Si back bonds.

VI. DISCUSSION AND CONCLUSIONS

It is clear that many defects can arise when H complexes with carbon. Substitutional carbon can weakly bind a single H atom, leading to a bistable electrically active center and which can be associated with the *E*3 and *H*1 DLTS lines. The H atom lies in a bond centered site for the neutral and positive defects, but is antibonded to C in the negative charge state. The binding energy of neutral H to C_s was calculated to be around 1.01 eV, in good agreement with other theoretical calculations, and is lower in the charged defects. This result seems to conflict with experimental results that have been interpreted in terms of a low activation energy for dissociation of the neutral species. On the other hand, if the neutral defect was a negative-*U* one, then two electrons would be trapped and lead to a structural change.

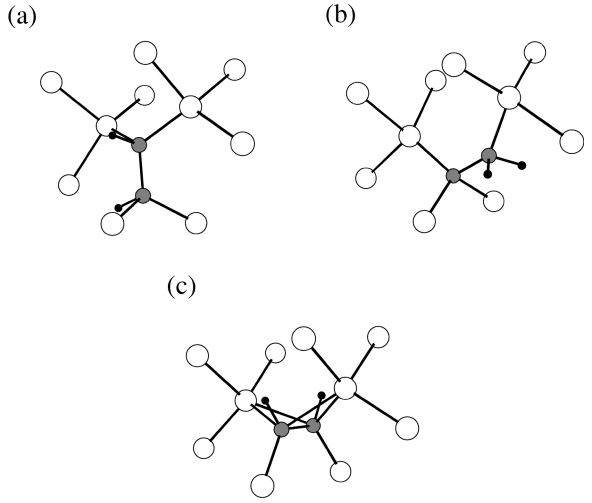

FIG. 11. The possible structures for the C_2-H_2 split-interstitial defect: (a) the $(C_2H_2)_{\langle 100\rangle}$ configuration, (b) the $(C_2H_2)_{BC}$ configuration, and (c) the $(C_2H_2)_{\langle 110\rangle}$ configuration.

We then considered the effect of adding a second hydrogen atom which leads to a stable electrically inactive H_2^* center. The two most likely configurations, $(C_sH_{BC})(SiH_{AB})$ and $(H_{AC}C_s)(H_{BC}Si)$, possessed almost identical energies, although their LVM's are quite different. There have been no reports of this center.

We then considered the defects formed when H interacts with C_i. The binding energy of H with C_i is very large, ~2.8 eV, and consequently such defects should be readily formed in irradiated material or annealed Czochralski (Cz) -Si. The neutral defect exists in two almost degenerate structures consisting of a $\langle 100\rangle$-oriented pair and a bond-centered pair. The bond-centered form has a similar structure to O_i. Its migration barrier is 0.4 eV, and this low value implies that the defect would easily migrate through the lattice readily forming complexes. The center is electrically active with a singly occupied level in the band gap. The negative charge center is stable in the bond-centered form, while the $\langle 100\rangle$ form is favored in the positive charge state.

The binding energy of C_iH with C_s is 0.6 eV, and the resulting $\langle 100\rangle$-oriented C-C pair, with H bonded with one C radical, is identified with the *T* photoluminescent (0.9351 eV) center. The calculated local vibrational modes and their isotope shifts are in good agreement with observations on this center. The formation of the *T* center by this reaction is more likely than the pairing of H with a dicarbon defect as the latter is not stable beyond ~300 °C. The *T* center can be

TABLE X. The calculated vibrational modes cm^{-1}, and isotope shifts for the $(C_2H_2)_{\langle 100\rangle}$ interstitial defect. The observed and calculated LVM's for the native IH_2 defect are also given for comparison.

Symmetry	$^{12}C\,^{12}CHH$	$^{12}C\,^{12}CHD$	$^{12}C\,^{12}CDD$	$^{12}C\,^{13}CHH$	$^{13}C\,^{13}CHH$
A	2995.6	2992.6	2196.8	2993.6	2987.1
B	2989.6	2196.1	2195.5	2982.6	2980.8
A	1226.6	1223.7	926.1	1224.3	1221.4
B	1220.9	895.6	882.9	1218.6	1216.8
B	1039.8	1043.1	1046.4	1022.6	1006.8
A	1000.0	993.7	743.0	998.7	997.6
B	976.7	741.3	722.3	973.8	969.1
A	633.5	616.1	601.7	628.1	615.2
B	631.4	612.8	599.9	619.2	613.1
A	560.2	557.4	555.3	556.1	552.8
IH_2 observed [a]	HH		HD		DD
A	1989.4				
B	1986.5				
	748.0				
	743.1				
IH_2 calculated [a]	HH		HD		DD
A	2154.3		2151.7		1546.6
B	2148.9		1544.5		1542.3
B	798.4		795.4		621.2
A	792.6		769.0		608.6

[a]Reference 46.

observed when CZ-Si is annealed to 450 °C, or when H-soaked float zone (FZ) -Si containing C is irradiated and subsequently annealed around 450 °C. The annealing is probably necessary to break up H molecules and silicon interstitial aggregates.

The C_i-H center can be passivated by further H trapping. Such a center would be immobile and its formation would block the production of *T* centers. Alternatively, *T* centers themselves could trap a second H, atom forming the inert C_s-C_i-H_2 defect.

There are of course many other possible defects formed, which are beyond the scope of this current work, among these are the reaction of the migrating C_i-H with O, N, and other CH defects. It seems likely that CH forms very similar defects to those of isoelectronic impurities such as N or P. For example, we have already pointed out that the C-CH pair is isoelectronic with C_i-P_s. More recent work[59] has showed that a N_iO_{2i} defect is a candidate for the shallow thermal donor, and if N is replaced by CH, there is little change in the structural or electronic properties.

ACKNOWLEDGEMENTS

We are grateful to A. N. Safonov, E. C. Lightowlers, and G. Davies for many useful discussions in relation to this work. We thank the HPCI for computer time on the T3D, where some of this work was carried out. S.Ö. thanks NFR and TFR in Sweden for financial support, and also PDC at KTH for computer time on the SP2.

[1] R. W. Series and K. G. Barraclough, J. Cryst. Growth **60**, 212 (1982).

[2] G. Davies, and R. C. Newman, in *Handbook on Semiconductors*, edited by S. Mahajan (Elsevier, Amsterdam, 1994), Vol. 3, p. 1557.

[3] M. J. Binns, S. A. McQuaid, R. C. Newman, and E. C. Lightowlers, Semicond. Sci. Technol. **8**, 1908 (1993).

[4] Y. Kamiura, M. Tsutsue, M. Hayashi, Y. Yamashita, and F. Hashimoto, Mater. Sci. Forum **196-201**, 903 (1995).

[5] A. N. Safonov, E. C. Lightowlers, G. Davies, P. Leary, R. Jones, and S. Öberg, Phys. Rev. Lett. **77**, 4812 (1996).

[6] R. C. Newman and J. B. Willis, J. Phys. Chem. Solids **26**, 373 (1965).

[7] R. C. Newman and R. S. Smith, J. Phys. Chem. Solids **30**, 1943 (1969).

[8] D. Windisch and P. Becker, Philos. Mag. A **58**, 435 (1988).

[9] P. A. Stolk, D. J. Eaglesham, H. J. Gossman, and J. M. Poate, Appl. Phys. Lett. **66**, 1370 (1995).

[10] A. R. Bean and R. C. Newman, Solid State Commun. **8**, 175 (1970).

[11] C. Kaneta, T. Sasaki, and H. Katayamayoshida, Phys. Rev. B **46**, 13 179 (1992).
[12] H. Yamanaka, Jpn. J. Appl. Phys. **6A**, 3319 (1994).
[13] R. Jones, J. Phys. C **20**, L713 (1987).
[14] R. Jones and S. Öberg, Semicond. Sci. Technol. **7**, 27 (1992).
[15] C. Kaneta and H. Katayama-Yoshida, in *The Physics of Semiconductors*, edited by D. J. Lockwood (World Scientific, Singapore, 1995).
[16] G. D. Watkins in, *Radiation Damage in Semiconductors*, edited by P. Barach (Dunod, Paris, 1964), p. 97.
[17] L. C. Kimberling, P. Blood, and W. M. Gibson, Inst. Phys. Conf. Ser. **46**, 273 (1978).
[18] L. W. Song and G. D. Watkins, Phys. Rev. B **42**, 5759 (1990).
[19] G. D. Watkins and K. L. Brower, Phys. Rev. Lett. **36**, 1329 (1976).
[20] J. F. Zheng, M. Stavola, and G. D. Watkins, in *The Physics of Semiconductors*, edited by D. J. Lockwood (World Scientific, Singapore, 1994) , p. 2363.
[21] R. Wooley, E. C. Lightowlers, A. K. Tipping, M. Claybourn, and R. C. Newman, Mater. Sci. Forum **10-12**, 929 (1986).
[22] S. K. Tipping and R. C. Newman, Semicond. Sci. Technol. **2**, 315 (1987).
[23] M. Besson and G. G. DeLeo, Phys. Rev. B **43**, 4028 (1991).
[24] M. J. Burnard and G. G. DeLeo, Phys. Rev. B **47**, 10 217 (1993).
[25] J. Tersoff, Phys. Rev. Lett. **64**, 1757 (1990).
[26] R. B. Capaz, A. Dal Pino, Jr., and J. D. Joannopoulos, Phys. Rev. B **50**, 7439 (1994).
[27] A. Mainwood, Mater. Sci. Forum **196-201**, 1589 (1995).
[28] R. Jones, S. Öberg, P. Leary, and V. J. B. Torres, Mater. Sci. Forum **196-201**, 785 (1995).
[29] P. Leary, R. Jones, S. Öberg, and V. J. B. Torres, Phys. Rev. B **55**, 2188 (1997).
[30] L. W. Song, X. D. Zhan, B. W. Benson, and G. D. Watkins, Phys. Rev. B **42**, 5765 (1990).
[31] K. P. O'Donnell, K. M. Lee, and G. D. Watkins, Physica B **116**, 258 (1983).
[32] X. D. Zhan and G. D. Watkins, Phys. Rev. B **47**, 6363 (1993).
[33] R. Jones and S. Öberg, Phys. Rev. Lett. **68**, 86 (1992).
[34] C. P. Ewels, R. Jones, and S. Öberg, in *Early Stages of Oxygen Precipitation in Silicon*, Vol. 17 of *NATO Advanced Study Institute, Series 3, High Technology*, edited by R. Jones (Kluwer, Dordrecht, 1996), p. 141.
[35] S. J. Pearton, J. W. Corbett, and M. Stavola, *Hydrogen in Crystalline Semiconductors* (Springer-Verlag, Berlin, 1992).
[36] K. Murakami, N. Fukata, S. Sasaki, K. Ishioka, M. Kitajima, S. Fujimura, J. Kikuchi, and H. Haneda, Phys. Rev. Lett. **77**, 3161 (1996).
[37] R. E. Pritchard, M. J. Ashwin, R. C. Newman, J. H. Tucker, E. C. Lightowlers, M. J. Binns, R. Falster, and S. A. McQuaid, Phys. Rev. B (to be published).
[38] A. N. Safonov and E. C. Lightowlers, Mater. Sci. Forum **143-147**, 903 (1994).
[39] E. C. Lightowlers, R. C. Newman, and J. H. Tucker, Semicond. Sci. Technol. **9**, 1370 (1994).
[40] E. C. Lightowlers, Mater. Sci. Forum **196-201**, 817 (1995).
[41] B. Holm, K. B. Nielsen, and B. B. Nielson, Phys. Rev. Lett. **66**, 2360 (1991).
[42] Y. V. Gorelinskii and N. N. Nevinnyi, Physica B **170**, 155 (1991).
[43] Y. Kamiura, Y. Nishiyami, anf F. Hashimoto, in *Diffusion in Materials*, edited by M. Koiwa, K. Hirano, H. Nakajima, and T. Okada (Trans Tech, Zurich, 1993), Vol. 95–98, p. 1001.
[44] Y. V. Gorelkinski and N. N. Nevinnyi, Mater. Sci. Eng. B **36**, 133 (1996).
[45] J. B. Holbech, B. Bech Nielsen, R. Jones, P. Sitch, and S. Öberg, Phys. Rev. Lett. **71**, 875 (1993).
[46] M. Budde, B. Bech Nielsen, P. Leary, J. Goss, R. Jones, P. R. Briddon, S. Öberg, and S. J. Breuer, Phys. Rev. B (to be published).
[47] S. M. Myers, Rev. Mod. Phys. **64**, 559 (1992).
[48] E. O. Sveinbjörnsson and O. Engström, Phys. Rev. B **52**, 4884 (1995).
[49] C. G. Van de Walle, P. J. H. Denteneer, Y. B. Yam, and S. T. Pantelides, Phys. Rev. B **39**, 10 791 (1989).
[50] A. Endroös, Phys. Rev. Lett. **63**, 70 (1989).
[51] Y. Kamiura, M. Yoneta, Y. Nishiyami, and F. Hashimoto, J. Appl. Phys. **72**, 3394 (1992).
[52] Y. Kamiura, M. Tsutsue, Y. Yamashita, and F. Hashimoto, J. Appl. Phys. **78**, 4478 (1995).
[53] D. M. Maric, P. F. Meier, and S. K. Estreicher, Phys. Rev. B **47**, 3620 (1993).
[54] Y. Zhou, R. Luchsinger, P. F. Meier, H. U. Suter, Dj. Maric, and S. K. Estreicher, Mater. Sci. Forum **196-201**, 891 (1995).
[55] C. Kaneta and H. Katayama-Yoshida, Y. Kamiura, M. Tsutsue, M. Hayashi, Y. Yamashita, and F. Hashimoto, Mater. Sci. Forum **196-201**, 897 (1995).
[56] N. S. Minaev and A. V. Mudryi, Phys. Status Solidi A **68**, 561 (1981).
[57] E. Irion, N. Burger, K. Thonke, and R. Sauer, J. Phys. C **8**, 5083 (1985).
[58] A. N. Safonov, E. C. Lightowlers, and G. Davies, Mater. Sci. Forum **196-201**, 909 (1995).
[59] C. P. Ewels, R. Jones, S. Oberg, J. Miro, and P. Deak, Phys. Rev. Lett. **77**, 865 (1996).
[60] R. C. Newman, J. H. Tucker, N. G. Semialtianos, E. C. Lightowlers, T. Gregorkiewicz, I. S. Zevenbergen, and C. A. J. Ammerlaan, Phys. Rev. B **54**, 6803 (1996).
[61] J. Weber and D. I. Bohne, in *Early Stages of Oxygen Precipitation in Silicon* (Ref. 34), p. 123.
[62] R. Jones and P. R. Briddon, in *Identification of Defects in Semiconductors*, edited by M. Stavola, Semiconductors and Semimetals, treatise editors R. K. Willardson, A. C. Beer, and E. R. Weber (Academic, New York, in press).
[63] G. B. Bachelet, D. R. Hamann, and M. Schlüter, Phys. Rev. B **26**, 4199 (1982).
[64] R. Jones, J. Phys. C **20**, 271 (1987).
[65] B. Bech Nielsen, L. Hoffmann, M. Budde, R. Jones, J. Goss, and S. Öberg, Mater. Sci. Forum **196-201**, 933 (1995).
[66] R. Jones, J. P. Goss, C. Ewels, and S. Öberg, Phys. Rev. B **50**, 8378 (1994).
[67] P. Deak, L. C. Snyder, M. Heinrich, C. R. Ortiz, and J. W. Corbett, Physica B **170**, 253 (1991).
[68] C. G. Van de Walle and J. Neugebauer, Phys. Rev. B **52**, 14 320 (1995).